

NUMERICAL STUDY OF THE JOHNSTON–OGSTON EFFECT IN TWO-COMPONENT SYSTEMS

John J. CORREIA[★], Michael L. JOHNSON^{★★}, George H. WEISS[◇], and David A. YPHANTIS[★]

Numerical solutions of the Lamm equation are presented for systems exhibiting the Johnston–Ogston effect. From these solutions it is apparent that the movement of the maxima of the concentration gradient curves reflects the sedimentation velocity of the slow or fast components in their appropriate plateaus. A simple generalization of the Johnston–Ogston analysis is presented, valid for all centrifugation times in a radial field and sector shaped cell provided only that there exist both a plateau of the slow component by itself and the mixed plateau with both slow and fast components present.

1. Introduction

One of the classical anomalies of velocity ultracentrifugation was first successfully explained by Johnston and Ogston, [1], although observed for more than a decade before, [2–4]. This anomaly, now known as the Johnston–Ogston effect, is manifest in a multicomponent system as an apparent increase in the amount of the less rapidly sedimenting components (with a corresponding decrease in the apparent amount of the faster components) during the sedimentation of mixtures. The effect vanishes at low solute concentrations and always increases with increasing concentrations. It is clear that this effect has its origin in the retardation of a slowly sedimenting solute by the presence of a more rapidly sedimenting solute.

A simple quantitative analysis was proposed by Johnston and Ogston [1] assuming a homogeneous field in a rectangular cell. This analysis was extended to a radially varying field and sector cell by Harrington and Schachman [5] and by Trautman et al. [6] but only for the beginning of the experiment when $t \rightarrow 0$.

These later publications also associate the existence of significant negative concentration gradients (and resultant convection) with the presence of the J–O effect.

Fujita [7] presents a calculated concentration distribution for a system exhibiting the J–O effect assuming (a) that diffusion is absent, and (b) that the sedimentation coefficients for both fast and slow components decrease linearly with the concentrations of the fast component. A salient feature of his calculation is the existence of a strong negative concentration gradient of the slow component, centripetal to the boundary of the fast component, as deduced by Harrington and Schachman [5] from their experimental observations.

We present here accurate numerical solutions of the Lamm equation for systems exhibiting the J–O effect. We also generalize the simple quantitative treatment of Johnston and Ogston [1] so as to become valid for radially varying field and sector cells and for all centrifugation times, provided only that there exists a plateau of the slow component by itself as well as a plateau with both fast and slow components present.

2. Discussion of numerical solutions

In what follows we restrict our analysis to systems with two sedimenting components in which the sedimentation coefficients depend on concentrations in the following way

[★] Biochemistry and Biophysics Section, Biological Sciences Group and Institute of Materials Science, University of Connecticut, Storrs, Connecticut 06268.

^{★★} Present address: Department of Biochemistry, University of Virginia Medical School, Charlottesville, Virginia 22904.

[◇] Physical Sciences Laboratory, Division of Computer Research and Technology, National Institutes of Health, Bethesda, Maryland 20014.

$$s_i(c_1, c_2) = s_i^0 / (1 + k_{i1}c_1 + k_{i2}c_2)$$

$$= s_i^0 f_i(c_1, c_2), \quad i = 1, 2, \quad (1)$$

where the s_i^0 are the sedimentation coefficients at infinite dilution. The Lamm equations to be solved are

$$\frac{\partial c_i}{\partial t} = \frac{1}{r} \frac{\partial}{\partial r} \left(r D_i \frac{\partial c_i}{\partial r} - r^2 \omega^2 s_i c_i \right), \quad i = 1, 2, \quad (2)$$

where the values of $\sigma_i \equiv \omega^2 s_i^0 / D_i = 117.4 \text{ cm}^{-2}$ are assumed equal and independent of concentration. This value of σ corresponds to the sedimentation of a protein of molecular weight $\sim 300\,000$ at $60\,000 \text{ rpm}$. Solutions to the Lamm equation were generated by the finite difference method described in detail by Dishon, Weiss, and Yphantis [8]. The original program was modified for the present problem to allow for two concentrations. Computation time for typical runs on an IBM 360/65 was between 40 minutes and an hour.

Fig. 1 presents the concentration profiles observed for a typical case where the sedimentation coefficients at zero concentration differ considerably ($s_2^0 = 2s_1^0$). This figure illustrates the clear separation into three regions, α , in which there is no solute present, β with an apparent plateau consisting of the slow component,

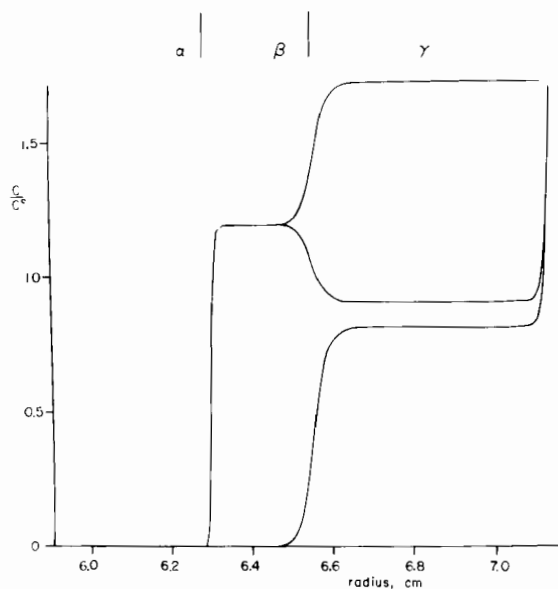


Fig. 1. Concentration profiles for individual components and for the total concentration at $\tau_1 = 0.3$. The parameter values are $c_1^0 = c_2^0 = 1$, $\sigma = 117.4 \text{ cm}^{-2}$, $s_1 = s_1^0 / (1 + c_1 + c_2)$, $s_2 = 2s_1^0 / (1 + c_1 + c_2)$.

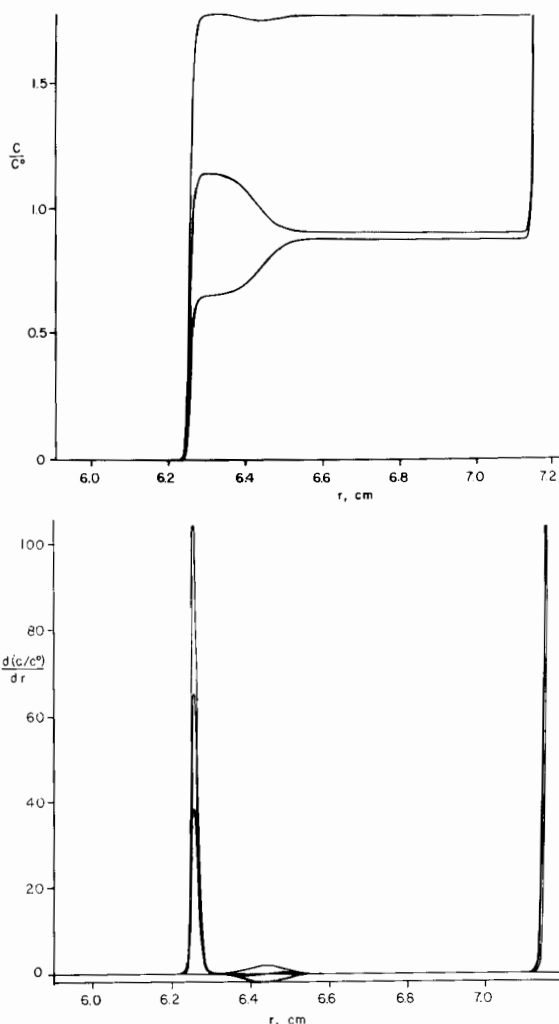


Fig. 2. (a) Concentration profiles of the individual components and of the total concentration for $\tau = 0.2$, $c_1^0 = c_2^0 = 1$, $s_1 = s_1^0 / (1 + c_2)$, $s_2 = 1.3s_1^0 / (1 + c_1)$. (b) Concentration gradients for the same parameters.

and γ with a true plateau with both fast and slow components. This standard demarcation into zones [6] will be used in the following presentation. The general features of the J-O effect that are apparent from this figure are: (1) an increase of the β plateau even above the loading concentration, compared to a plateau concentration of ~ 0.86 expected for these conditions in the absence of the fast component; and (2) a marked sharpening of the $\alpha\beta$ boundary in comparison with the minimal sharpening of the $\beta\gamma$ boundary. This relative sharp-

ening is understandable in terms of the relative decrease of sedimentation coefficients across the $\alpha\beta$ and $\beta\gamma$ boundaries. These are

$$(s_{1\beta} - s_{1\alpha})/s_{1\beta} = 1.2, \quad (s_{1\gamma} - s_{1\beta})/s_{1\beta} = 0.2. \quad (3)$$

Fig. 2 presents a rather extreme case of the J–O effect for $k_{11} = k_{22} = 0, k_{12}c_2^0 = k_{21}c_1^0 = 1$, in which self-concentration dependence is absent and only cross dependence present. This unnatural case shows an almost complete compensation of the fast and slow components in the fast boundary. The only trace of this boundary is seen as a small perturbation of the calculated schlieren curve. Again, the substantial sharpening of each of the slow boundaries relative to their fast boundaries is evident. It is interesting to note that both boundaries are mixed, with considerable amounts of both components present. It is also interesting to note that there is a region with a marked total negative concentration gradient. This total negative concentration gradient is even more pronounced in the curve of the concentration gradients in fig. 3b for the case $k_{21} = k_{22} = k_{11} = 0, k_{12}c_2^0 = 1$. The complementary case where $k_{21}c_1^0 \neq 0, k_{11} = k_{22} = 0$ also exhibits a large negative concentration gradient during the time that the boundaries of both components interact.

We now restrict ourselves to the more natural case in which $k_{11}c_1^0 = k_{12}c_2^0 = k_{21}c_1^0 = k_{22}c_2^0 = A$, where A will take on different values. Fig. 4a for $A = 1$ shows total concentration gradients calculated for $\tau_1 = 2\omega^2s_1^0t = 0.1, 0.2$, and 0.3 and for $s_2^0 = 1.3s_1^0$. A marked J–O effect is obvious. The $\alpha\beta$ and $\beta\gamma$ boundaries are not clearly resolved making difficult the estimation of the apparent amount of the fast component. In such cases we estimate the apparent amount of the fast component by assuming the concentration gradient of the faster boundary to be symmetric about its maximum. In fig. 4b we present values of the individual and total concentration gradients at $\tau_1 = 0.3$ for $A = 0.5$ and $s_2^0 = 1.3s_1^0$. Here the resolution of the two boundaries is improved.

The quantitative aspects of the J–O effect are illustrated in fig. 5 which presents the apparent amounts of the fast component that would be estimated using the following procedures: The estimated or observed areas under the gradient curves in the $\beta\gamma$ boundaries were corrected for radial dilution (by multiplication by $(r_{\beta\gamma}^*/r_0)^2$, where $r_{\beta\gamma}^*$ is the radial position of the maximum gradient in the $\beta\gamma$ boundary and r_0 is the

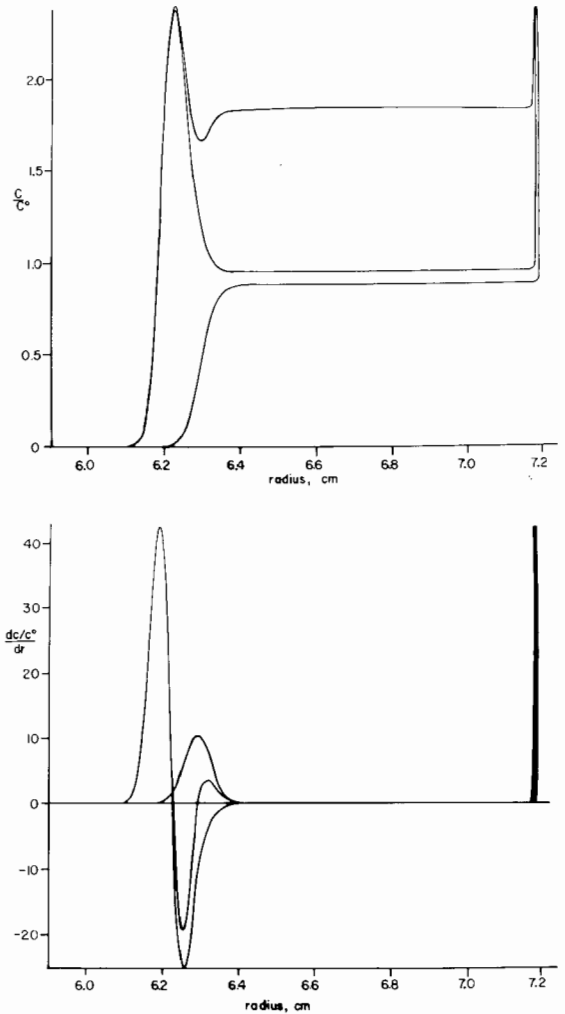


Fig. 3. (a) Individual and total concentration profiles for $\tau = 0.1, c_1^0 = 1, s_2 = 1.3s_1^0, s_1 = s_1^0/(1 + c_2)$. (b) Concentration gradients for the same parameters.

meniscus radius) and averaged over τ . Two sets of observations are shown as points for $s_2^0 = 1.3s_1^0$ and $2s_1^0$, and for several values of A . The curves correspond to the predictions of Johnston and Ogston [1] for a rectangular system or of Harrington and Schachman [5], and of Trautman et al. [6] for zero time with radial field and sector cell. The agreement between these predictions and our calculations is quite good for $s_2^0 = 2s_1^0$; the deviations seen for $s_2^0 = 1.3s_1^0$ probably reflect our difficulties in estimating the total areas corresponding to the incompletely resolved $\beta\gamma$ boundaries. These boundaries are clearly asymmetric when $s_2^0 = 2s_1^0$,

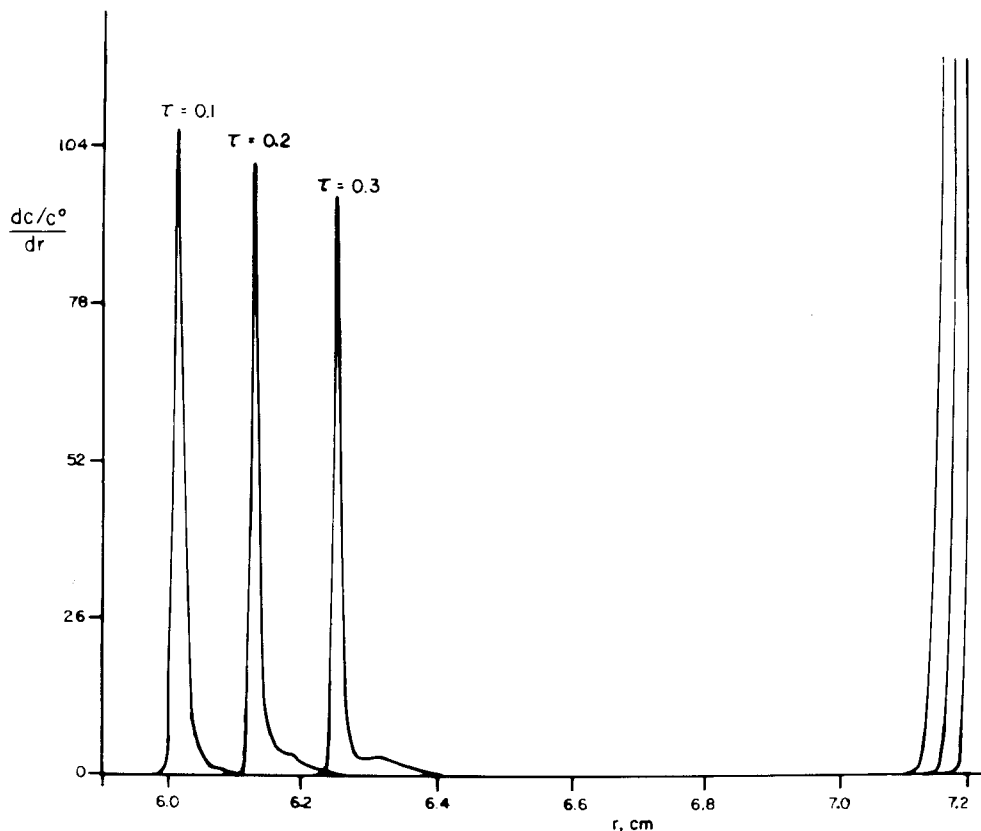


Fig. 4. (a) Total concentration gradients for $\tau = 0.1, 0.2, 0.3$, $c_1^0 = c_2^0 = 1$, $s_1 = s_1^0/(1 + c_1 + c_2)$, $s_2 = 1.3s_1^0/(1 + c_1 + c_2)$.

and are expected to be even more asymmetric when the sedimentation coefficients differ less and the boundaries overlap more.

It should be noted that the data in fig. 5 for small concentration dependence extrapolate linearly to zero concentration. This tends to substantiate the usual practice of linearly extrapolating to zero loading concentration the apparent amounts of components estimated in sedimentation velocity experiments. However caution needs to be exercised for concentration coefficients A greater than about 0.2, in this particular model.

3. Derivation of relations

The simple relation of Johnston and Ogston [1] for

the rectangular system or of Harrington and Schachman [5] and Trautman et al. [6] for zero time, that appears to predict the corrected apparent amounts of components can be shown to be valid for a radial field in a sector shaped cell without restricting the time, provided both the β and γ plateaus exist. The argument is based on conservation of mass. Consider the rate of transport of the slow component across two radii r_β and r_γ in the two plateaus:

$$\left. \frac{dQ}{dt} \right|_{r_\beta} = \theta h r_\beta J_1(r_\beta) = \theta h \omega^2 s_1^\beta c_1^\beta r_\beta^2, \quad (4)$$

$$\left. \frac{dQ}{dt} \right|_{r_\gamma} = \theta h r_\gamma J_1(r_\gamma) = \theta h \omega^2 s_1^\gamma c_1^\gamma r_\gamma^2,$$

where θ and h are, respectively, the sector angle and thickness of the ultracentrifuge cell, c_1^β and c_1^γ are the

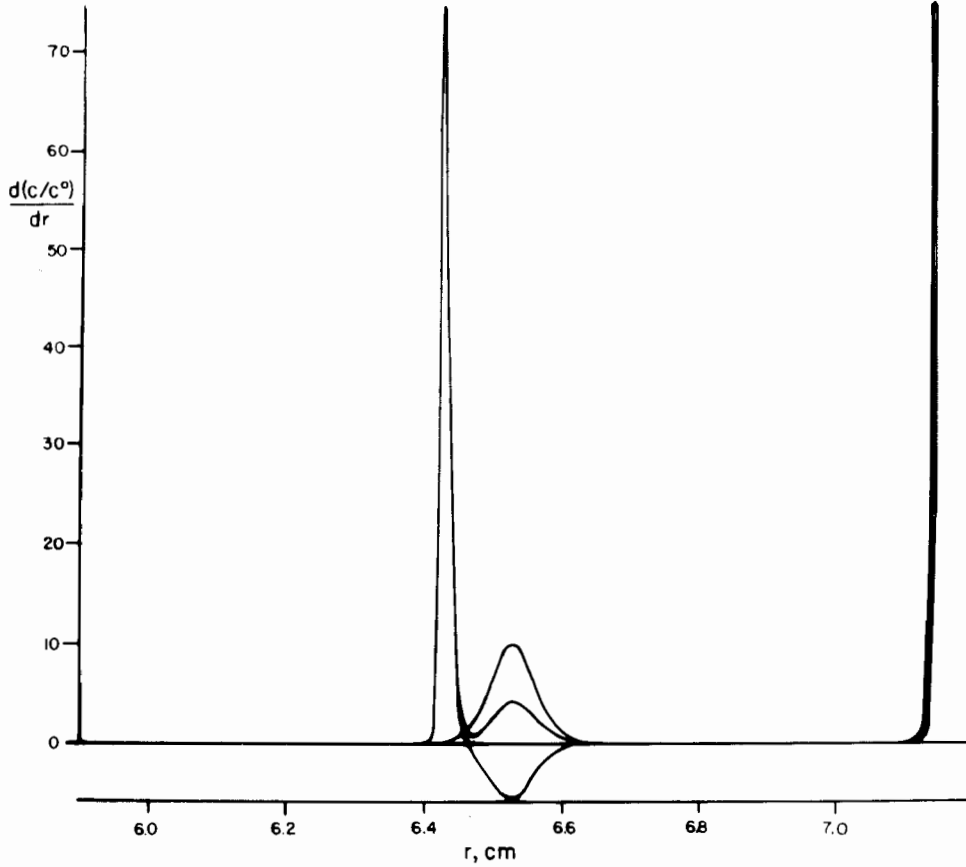


Fig. 4. (b) Individual and total concentration gradients for $\tau = 0.3$, $c_1^0 = c_2^0 = 1$, $s_1 = s_1^0/(1 + 0.5c_1 + 0.5c_2)$ and $s_2 = 1.3s_1^0/(1 + 0.5c_1 + 0.5c_2)$.

concentrations in the β and γ plateaus, and where $J_1(r)$ is the flow of the slow component at any radius r . We further define an equivalent radius, r_e , by the condition that

$$2Q_{\beta\gamma}/\theta h = c_1^\beta(r_e^2 - r_\beta^2) + c_1^\gamma(r_\gamma^2 - r_e^2) = 2 \int_{r_\beta}^{r_\gamma} c_1 r dr, \quad (5)$$

where $Q_{\beta\gamma}$ is the amount of slow component between r_β and r_γ . In other words r_e is the position of the infinitely sharp boundary between the two uniform plateaus (at c_1^β and c_1^γ) that conserves the mass of component 1 between r_β and r_γ . Consider now the flux of component 1 in the region $r_\beta \leq r \leq r_\gamma$,

$$\frac{dQ_{\beta\gamma}}{dt} = \frac{1}{2} \theta h \left((r_e^2 - r_\beta^2) \frac{dc_1^\beta}{dt} + (r_\gamma^2 - r_e^2) \frac{dc_1^\gamma}{dt} + \right.$$

$$\left. + 2(c_1^\beta - c_1^\gamma)r_e \frac{dr_e}{dt} \right) = \frac{dQ_\beta}{dt} - \frac{dQ_\gamma}{dt} = \theta h \omega^2 (s_1^\beta c_2^\beta r_\beta^2 - s_1^\gamma c_1^\gamma r_\gamma^2). \quad (6)$$

Substituting the time rates of change of the plateau concentrations as

$$\frac{dc_1^\beta}{dt} = -2\omega^2 s_1^\beta c_1^\beta, \quad \frac{dc_1^\gamma}{dt} = -2\omega^2 s_1^\gamma c_1^\gamma \quad (7)$$

in this last equation we obtain

$$(s_1^\beta c_1^\beta - s_1^\gamma c_1^\gamma) = (c_1^\beta - c_1^\gamma) \frac{d \ln r_e}{\omega^2 dt} = (c_1^\beta - c_1^\gamma) s_e, \quad (8)$$

where $s_e \equiv (1/\omega^2) d \ln r_e / dt$ represents the sedimentation coefficient of the equivalent boundary at r_e . Thus in order to maintain the β plateau, with no net depletion

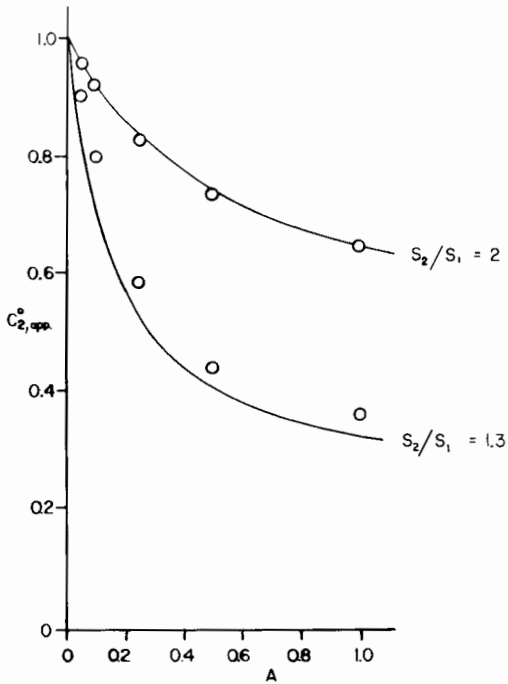


Fig. 5. Corrected apparent initial concentrations of the fast component obtained by correction for radial dilution of the observed or estimated areas of the fast boundaries (see text for details). The curves were calculated using the Johnston-Ogston equation. The concentration dependence is $A = k_{ij}c_j^0$ and $s_i = s_i^0/(1 + Ac_1/c_1^0 + Ac_2/c_2^0)$.

or accretion at the $\beta\gamma$ boundary, s_e must be given by

$$s_e = (c_1^\beta s_1^\beta - c_1^\gamma s_1^\gamma)/(c_1^\beta - c_1^\gamma). \quad (9)$$

Conversely, if the equivalent $\beta\gamma$ boundary moves with some sedimentation coefficient s_e then the value of the concentration in the β plateau must satisfy eq. (8) if the plateau is to be maintained. In particular, let us assume, as motivated by our numerical evaluations, that the sedimentation coefficient of the $\beta\gamma$ boundary is equal to s_2^γ , the sedimentation coefficient of the fast component in its plateau. Then we must have

$$c_1^\beta = c_1^\gamma (s_2^\gamma - s_1^\gamma)/(s_2^\gamma - s_1^\beta), \quad (10)$$

which is the relation inferred by others for their more restricted cases. Thus this relation is generally valid provided that both the β and the γ plateaus exist and provided that the $\beta\gamma$ boundary does indeed move with the velocity of the fast component.

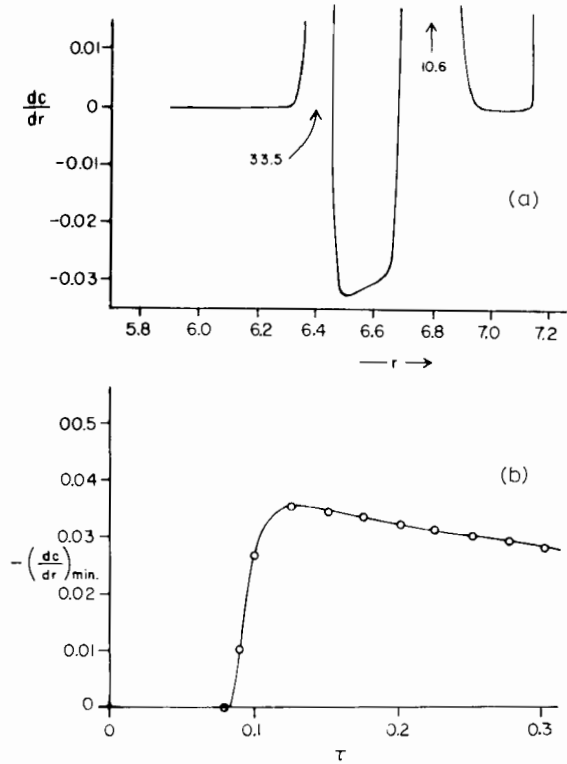


Fig. 6. (a) Calculated total concentration gradient presented on a magnified scale for $s_1 = s_1^0/(1 + 0.25c_1 + 0.25c_2)$, $s_2 = 2s_1^0/(1 + 0.25c_1 + 0.25c_2)$, $c_1^0 = c_2^0 = 1$ and $\tau = 0.2$. (b) Values of the maximum of the absolute value of the negative concentration gradient observed in the β region for the same parameters presented as a function of τ_1 .

4. Comparison between theory and numerical solutions

Let us now examine these premises. Fig. 6a presents a magnified view of the concentration gradients for a typical case. It is seen that there is a small negative concentration gradient in the " β -plateau", about 10^{-2} – 10^{-3} times the magnitude of the maximum gradients observed in the boundaries. This small negative concentration gradient decreases with time, after its initial generation, as shown in fig. 6b. The magnitude of the maximum absolute value of this gradient depends on A , and appears to be greatest for $0.25 < A < 0.5$ when all the k_{ij} are equal. On the basis of the limited number of cases that we have examined with s_2^0 differing from s_1^0 , the " β plateau" seems to have, at most, a small negative concentration gradient. This is illustrated for an extreme concentration dependence in fig. 7, where even

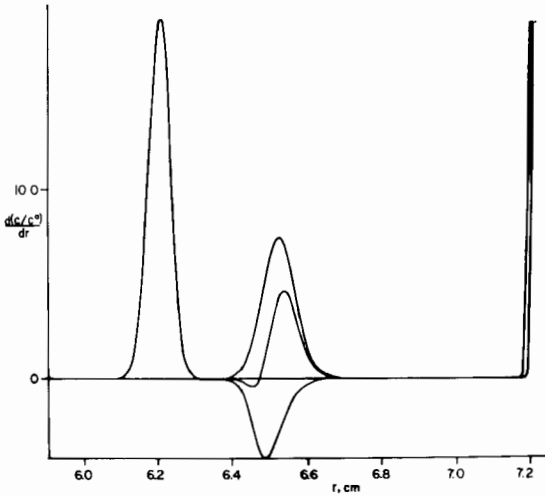


Fig. 7. Individual and total concentration gradients calculated for $\tau = 0.1$, $c_1^0 = c_2^0 = 1$, $s_1 = s_1^0/(1 + c_2)$ and $s_2 = 2s_1^0$.

the presence of a large negative total concentration gradient in the $\beta\gamma$ boundary leads to only small negative concentration gradients in the β region.

In order to test eq. (9) we require values of the γ plateau concentrations, c_i^γ . These can be obtained by solving the Lamm equations appropriate to this plateau:

$$\begin{aligned} \frac{dc_i^\gamma}{dt} &= -2\omega^2 s_i^\gamma c_i^\gamma \\ &= -2\omega^2 s_i^0 c_i^\gamma / (1 + k_{i1} c_1^\gamma + k_{i2} c_2^\gamma). \end{aligned} \quad (11)$$

To obtain a relation between c_1 and c_2 we divide eq. (11) for $i = 1$ by its counterpart for $i = 2$, finding

$$\frac{d \ln c_1^\gamma}{d \ln c_2^\gamma} = \frac{s_1^0}{s_2^0} \left(\frac{1 + k_{21} c_1^\gamma + k_{22} c_2^\gamma}{1 + k_{11} c_1^\gamma + k_{12} c_2^\gamma} \right). \quad (12)$$

For special cases this may be solved in closed form, but numerical integration of this equation appears to be necessary for its solution in the general case. If $k_{11} = k_{21}$, this equation reduces to

$$d \ln c_1^\gamma = (s_1^0/s_2^0) d \ln c_2^\gamma \quad (13a)$$

or

$$c_2^\gamma = K(c_1^\gamma)^{s_2^0/s_1^0}, \quad (13b)$$

where K is a constant. Combining eqs. (13) and (11) we find an ordinary differential equation for c_i^γ which must be solved numerically. Thus we obtain values of

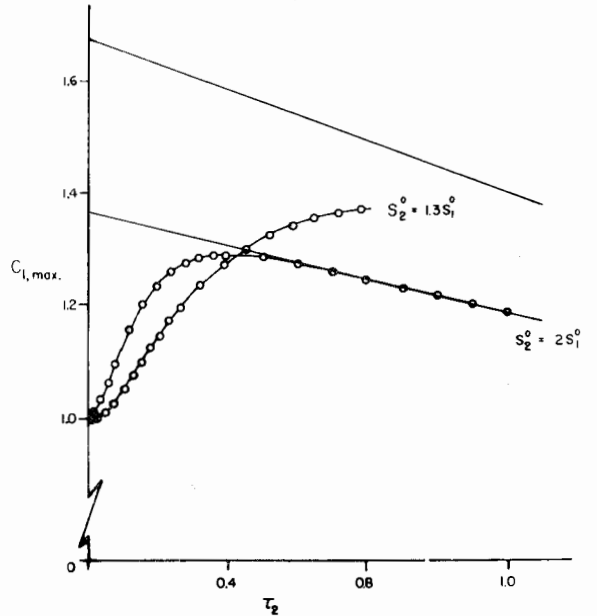
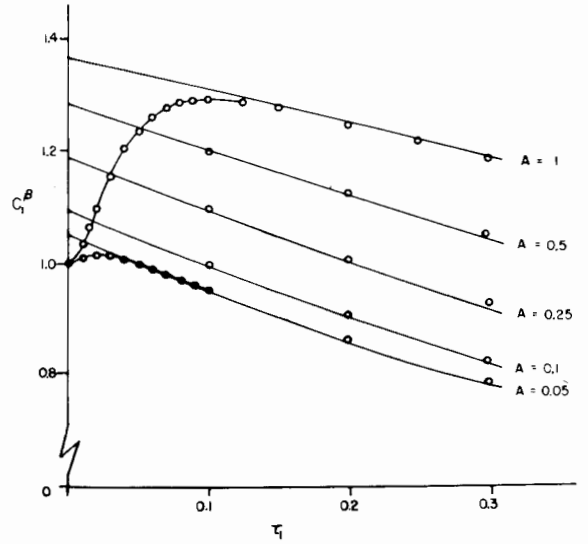


Fig. 8. (a) Concentrations in the β plateau as a function of τ_1 . The points indicate the maximum observed concentration in the β region and the curves were calculated as described in the text. The parameters used were $c_1^0 = c_2^0 = 1$, $s_2^0 = 2s_1^0$ and $s_i = s_i^0/(1 + Ac_1 + Ac_2)$. (b) Comparison of the concentrations observed and estimated for $s_2^0 = 1.3s_1^0$, $s_2^0 = 2s_1^0$ and for $A = 1$ presented as a function of $\tau_2 = 2\omega^2 s_2^0 t$.

c_i^γ for any t when the k_{ij} are equal. These now enable us to obtain estimates of c_1^β from eq. (10). Fig. 8a compares the observed c_1^β or, when a negative concentration gradient is significant, the maximum values of c_1^β

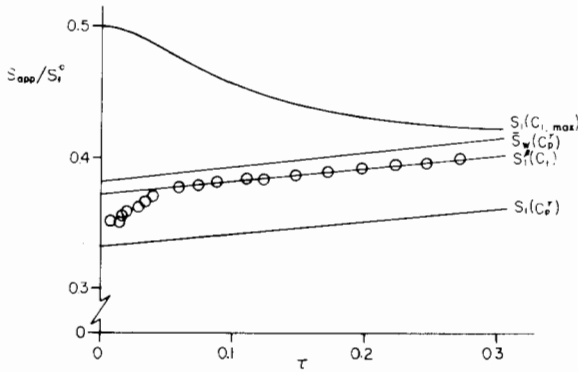


Fig. 9. Apparent sedimentation coefficients calculated from the rate of movement of the maximum gradient in the slow boundary presented as a function of time for $c_1^0 = c_2^0 = 1$, $s_2^0 = 1.3s_1^0$ and $s_i = s_i^0/(1 + c_1 + c_2)$. The curves represent the sedimentation coefficients calculated for the slow component at the maximum concentrations in the β region [$s_1(c_1 \max)$]; the weight average sedimentation coefficient in the γ plateau [$\bar{s}_w(c_p^\gamma)$]; the sedimentation coefficient of the slow component at the predicted β plateau concentration [$s_1(c_p^\beta)$]; and the sedimentation coefficient of the slow component in γ plateau [$s_1(c^\gamma)$].

with these predicted values of c_1^β for $s_2^0 = 2s_1^0$ as a function of τ_1 . The agreement is good after the $\alpha\beta$ and $\beta\gamma$ boundaries become distinct. The agreement is much poorer for $s_2^0 = 1.3s_1^0$ (fig. 8b), presumably because the boundaries are never separated.

Fig. 9 presents the apparent sedimentation coefficients calculated from the movement of the maximum concentration gradient in the $\alpha\beta$ boundary of our calculated distributions when $k_{ij} = 1$, and $s_2^0 = 1.3s_1^0$. For comparison, we have calculated the expected sedimentation coefficients for the maximum concentration in the β region, for the slow component and for the weight average of the components in the γ plateau, and for the predicted value of c_1^β . Clearly, the movement of the maximum gradient in this example corresponds to the sedimentation behavior expected for the non-existent β plateau. Another comparison of sedimentation coefficients from the maximum dc/dr in the $\alpha\beta$ boundary for $s_2^0 = 1.35s_1^0$ and $k_{ij} = 0.5$ is presented in fig. 10a. In this case, again, the movement of the slow boundary appears to be governed by the concentration of the fictitious β plateau. The sedimentation coefficient calculated from the rate of movement of the maximum gradient in the $\beta\gamma$ boundary for this case is presented in fig. 10b. It appears that the rate of movement cor-

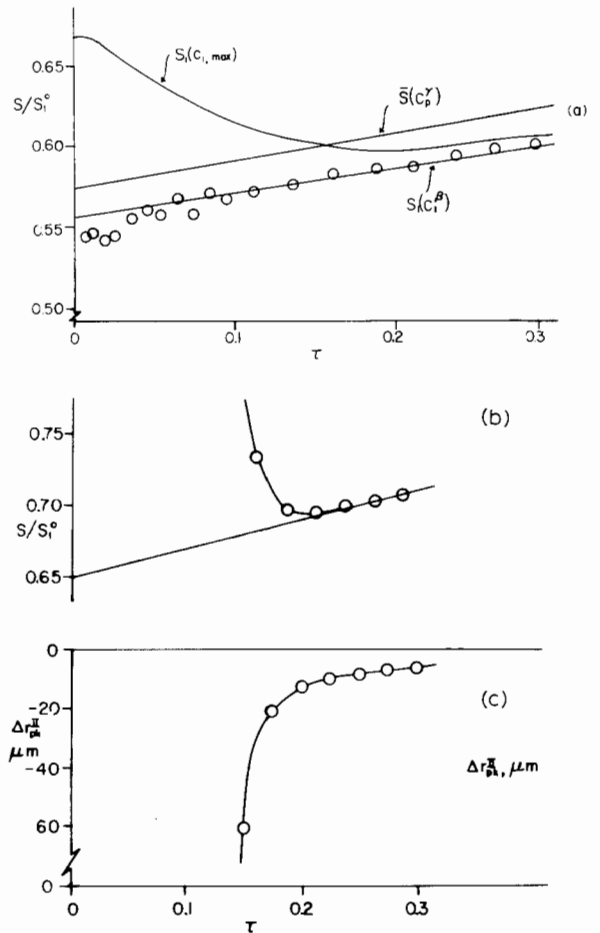


Fig. 10. Parameters: $c_1^0 = c_2^0 = 1$; $s_2^0 = 1.3s_1^0$; and $s_i = s_i^0/(1 + 0.5c_1 + 0.5c_2)$. A comparison of the observed sedimentation coefficients (corresponding to the movement of the maximum gradient in the slow boundary) with sedimentation coefficients predicted for the maximum concentration in the β region [$s_1(c_1 \max)$]; for the weight average sedimentation coefficient in the γ plateau [$\bar{s}_w(c_p^\gamma)$]; and for the slow component at the predicted β plateau concentration [$s_1(c_p^\beta)$]. (b) Comparison of the sedimentation coefficient calculated from the rate of movement of the maximum gradient in the fast boundary with the sedimentation coefficient calculated for the fast component in the γ plateau. (c) The difference in radius between the observed peak position of the concentration gradient curves and the position calculated for the equivalent boundary of the fast component in the γ plateau.

responds to the sedimentation coefficient in the γ plateau after the two boundaries have separated.

Fig. 10c also shows the differences between the

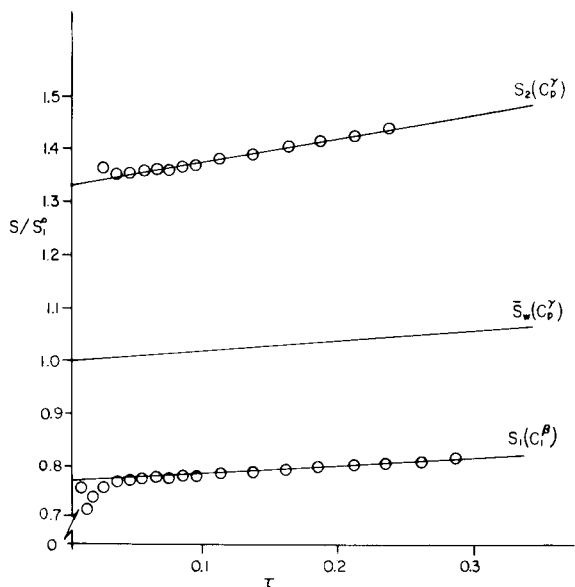


Fig. 11. Comparison of the sedimentation coefficient from movement of the maximum of the total dc/dr observed for the fast (top) and slow boundaries with the sedimentation coefficients $s_2(c_2^\gamma)$ and $s_1(c_1^\beta)$. Parameters: $c_1^0 = c_2^0 = 1$; $s_2^0 = 2s_1^0$; and $s_i = s_i^0/(1 + 0.25c_1 + 0.25c_2)$.

observed maximum gradient positions in the $\beta\gamma$ boundary and the positions calculated for the equivalent boundary corresponding to the γ -plateau concentration of the fast component, c_2^γ . The maximum gradient corresponds, asymptotically, to this equivalent boundary.

The agreement between observed and predicted sedimentation coefficients appears to be even better when the sedimentation coefficients of the fast and slow components are more disparate. Fig. 11 presents typical observations for $s_2^0 = 2s_1^0$ and $A = 0.25$, substantiating a general conclusion that the rates of movement of the maximum concentration gradients in the $\alpha\beta$ and $\beta\gamma$ boundaries closely reflect the values of the sedimentation coefficients $s_1(c_1^\beta)$ and $s_2(c_2^\gamma)$ respectively.

If the β -plateau exists it will maintain itself and the values of c_1^β can be simply predicted, independently of the behavior in the γ plateau, from solution of eq. (7) as

$$\ln c_1^\beta + \tau_1 = -k_{11}c_1^\beta + \ln c_1^\beta(\tau_1 = 0) + k_{11}c_1^\beta(\tau_1 = 0). \quad (14)$$

Thus a graph of $\tau_1 + \ln c_1^\beta$ vs c_1^β should be linear with

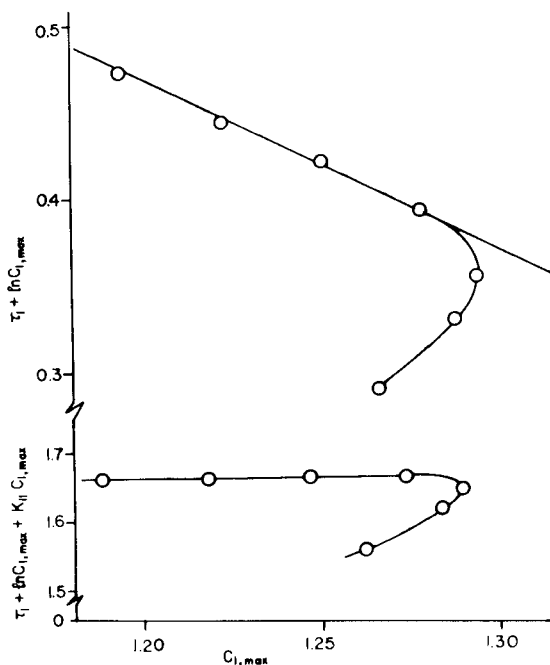


Fig. 12. Test of prediction of the behavior of the plateau concentration for $c_1^0 = c_2^0 = 1$; $s_2^0 = 2s_1^0$; and $s_i = s_i^0/(1 + c_1 + c_2)$. See the text for details. (a) Estimation of $-k_{11}$ as the slope of the linear segment of the curve. (b) Estimation of the initial concentration of the slow component.

slope $-k_{11}$. Such a graph is presented for $s_2^0 = 2s_1^0$ and $k_{ij} = 1$ in fig. 12, taking c_1^β as the maximum value of c_1 in the β region. The indicated line has been drawn with the expected slope of -1 . Addition of the term $k_{11}c_1^\beta$ to both sides of eq. (14) provides estimates of $G = \ln c_1^\beta + k_{11}c_1^\beta$ for $\tau = 0$ that should be independent of centrifugation time. Such estimates are presented in the lower portion of fig. 12. One sees that these values are constant after the initial separation of the boundaries and that the average value for G is 1.665 which corresponds to $c_1^\beta(0) = 1.359$. This value can be compared to the expected value of 1.366 calculated for c_1^β from eq. (10) when $c_1^\gamma = c_2^\gamma = 1$. A similar treatment of data for $k_{ij} = 0.25$ gives an estimate of $k_{11} = 0.215$, but the observed value of $G (= 0.423)$ obtained with this estimated k_{11} gives an estimated value of $c_1^\beta(0) = 1.184$, compared to the expected value of 1.186 obtained from eq. (10) with the true value of k_{11} and $c_1^\gamma = c_2^\gamma = 1$. Thus it appears that we can calculate the concentration in the β plateau from the initial value of c_1^β (at $t = 0$), given by the original Johnston–Ogston equation

for the initial concentrations loaded in the cell and from the form of the concentration dependence of the slow component by itself.

5. Conclusions

A simple theory of the J-O effect that generalizes the work of earlier investigators has been given. We have found, through an analysis of accurate solutions to the coupled Lamm equations, that when the peaks in a two component system have separated sufficiently, a relatively simple theory developed on the assumption of the existence of two plateaus leads to accurate qualitative and quantitative results. However, we have also found that the numerical solutions also predict very slight negative concentration gradients in the β region, almost certainly unobservable in practice and much smaller than the strong negative concentration gradients suggested by Fujita's calculation, [7]. It would be interesting to determine conditions on the concentration dependence of the sedimentation coefficients that would imply absolute plateaus (i.e., $\partial c_i / \partial r = 0$), and also to insure, for realistic choices of these coefficients, that any negative gradients would indeed be small. We have been unable to do this with any generality, but it is our feeling that real world parameters do not lead to difficulties related to substantial concentration gradients in the β region.

Acknowledgement

This work was supported, in part, by a grant from the National Science Foundation, #GB-30825X, and by Public Health Service Training Grant, #GM-00317. Numerical computations were performed at the University of Connecticut Computing Center, which has been supported, in part, by grant #GJ-9 from the National Science Foundation. We wish to thank Mr. Raymond Kikas and Mrs. Lorna Yphantis for their technical assistance.

References

- [1] J.P. Johnston and A.G. Ogston, *Trans. Faraday Soc.* 42 (1946) 789.
- [2] A.S. McFarlane, *Biochem. J.* 29 (1935) 407.
- [3] K.O. Pedersen, *Nature* 138 (1936) 363.
- [4] K.O. Pedersen, *Compt. Rend. Lab. Carlsberg* 22 (1938) 427.
- [5] W.F. Harrington and H.K. Schachman, *J. Am. Chem. Soc.* 75 (1953) 3533.
- [6] R. Trautman, V.N. Schumaker, W.F. Harrington and H.K. Schachman, *J. Chem. Phys.* 22 (1954) 555.
- [7] H. Fujita, *Mathematical Theory of Sedimentation Analysis* (Academic Press, New York and London, 1962).
- [8] M. Dishon, G.H. Weiss and D.A. Yphantis, *Biopolymers* 4 (1966) 449.